International Journal of Thin Films Science and Technology

http://dx.doi.org/10.18576/ijtfst/090308

Effect of the Synthesis Route on the Structural, Morphological and Dielectric Properties of Bi4 (Ni2/3,Ta1/3)0.08Ti2.92O12 Aurivillius Phases

H. Menasra[*], *K. Bounab, Z. Necira, A. Meklid and A. Boutarfaia*

Laboratory of Applied Chemistry, University of Biskra, Biskra, Algeria

Received: 16 Jul. 2020, Revised: 13 Aug. 2020, Accepted: 23 Aug. 2020.
Published online: 1 Sep. 2020.

Abstract: The effect of 8% of (Ni2+, Ta5+) content and the route of synthesis (i.e., conventional solid state reaction « CSS » and molten salt method « MS ») on micro-structural, morphological and dielectric properties of BIT ceramics have been investigated. X-ray diffraction (XRD) analysis revealed that the (Ni,Ta)- modified BIT ceramics have a pure orthorhombic three-layer Aurivillius type structure. Phase purity is obtained at 950°C by CSS reaction and by the MS method at 850°C. SEM/ EDX results confirms that the samples have a relatively dense pure, with micro-grains plate-like, structure typical for Aurivillius layered structures but strongly influenced by the crystallite size of both methods. The dielectric constant and the tangent loss of 8%-BNTT have been found to be decreasing by shifting the curie temperature to a high temperature, when we change the reaction from CSS to MS.
Keywords: Aurivillius phases, $Bi_4Ti_3O_{12}$, crystallite size, dielectric properties.

1 Introduction

For fifty years, an important research activity has been dedicated to the family of bismuth layer-structured ferroelectrics (abbreviated as BLSFs), which was discovered by Aurivillius in 1949 [1, 2]. Among them, the family of three-layered Aurivillius phase $Bi_4Ti_3O_{12}$ or (BIT) demonstrates the richness of this family because of their high Curie temperature (~ 675 °C) and fatigue-free properties, which makes it the favorite candidate for FRAM devices and piezoelectric sensors [3- 9]. The chemical structure of $B_4Ti_3O_{12}$ is $(Bi_2O_2)^{2+}(Bi_2Ti_3O_{10})^{2-}$ or $(Bi_2O_2)^{2+}(Bi_{m-1}Ti_{3m}O_{3m+1})^{2-}$ when m=3, where the anion site is a pseudoperovskite sandwiched between cation site along its axis cristallographic (c) [1]. To enhance the properties of the BIT ceramics, several dopants or co-dopants are used without changing the perovskite-like layer number m = 3 [10- 16]. For instance, Noguchi Y and al. [17] substitute the Bi-site with high valent ions (Nb^{5+}, V^{5+}, W^{6+}) but Hongchu Du and al. [18] co-doped the same site with La/ W, Mo, Nb, and V to reduce the oxygen vacancies and enhance the electrical properties. On the other hand, many researchers have co-doped the (Ti-site) with different pairs of ions such as (Fe^{3+}/Co^{3+}), (Fe^{3+}/Nb^{5+}), (Nb^{5+}/Ta^{5+}) and (W^{6+}/Cr^{3+}) to improve multiferroic properties and magnetoelectric coupling [19- 24]. According to the literature, the synthesis of BIT aurivillius was done by different preparation methods: sol-gel method [25, 26], Pucheni method [27, 28] and solid state reaction [29- 32].

2 Experimental Sections

2.1 Preparation of Ceramics

The aurivillius ceramics $Bi_4(Ni_{2/3}Ta_{1/3})_{0.08}Ti_{2.92}O_{12}$, (abbreviated as 8% BNTT) is prepared by conventional solid-state reaction (CSS) and molten salt method (MS). *Molten salt synthesis:* Reagent-grade Bi_2O_3 (99.99%), Ta_2O_5 (99.99%), NiO (99.99%) and TiO_2 (99.8%) were weighted according to the stoichiometric ratio and mixed together with the same weight of the mixture (NaCl/ KCl) (1/ 1). The choice of (NaCl / KCl) is based on the nature of the precursors and the protocol reported by Kimura, T. & Yamaguchi, T [38]. Then, the mixture was crushed in a mortar of a glass for 3 hours and calcined at 850°C for 4 hrs with a heating rate of 2°C/min. To assure the removal of residual salts, prepared products have been washed several times with hot water until no Cl^- was detected by the $AgNO_3$ solution.

*Corresponding author E-mail: h.menasra@univ-biskra.dz

Solide state reaction: The same high purity reagent grade component oxides in the desired stoichiometry have been thoroughly mixed in a mortar of a glass for about 4 hours. Then the mixed powder was calcined twice at the same temperature, 950°C, for 4 hrs with a speed of 2°C /min this confirms the formation of the Aurivillius phase without pyrochlore ($Bi_2Ti_2O_7$ ICSD : 98-009-9435) phases.

Finally to the two processes, cylindrical pellets of 13 mm diameter and 2 mm thickness were prepared under 2000 kg/cm^3 pressure. The pellets were, then, sintered at 900°C for 4 hrs.

2.2 Characterization of ceramics

The phase structure of the synthesized Product was characterized by X-ray diffraction (XRD), using BRUCKER-AXS type D8 ADVANCE with CuKα radiation (λ=1,5406° Å) in a wide range of Bragg angles (10°≤ 2θ≤ 70°), and the lattice parameters were calculated from the XRD data, using the cellref program, and the crystallite size (D) was estimated, using Debye–Scherrer's equation ($D_{sch.}$) and Williamsson-Hall method (*DW-H*) as follows [35, 39].

$$D_{sch} = \frac{k\times\lambda}{\beta\times\cos(\theta)} \quad (1)$$

$$\beta\cos(\theta) = \frac{k\times\lambda}{D_{W-H}} + 4\varepsilon\times\sin(\theta) \quad (2)$$

Where k= 0.9 is the shape factor, β is the full width at half maximum, and ε is the effective strain. Additionally, the elemental composition and morphological properties were esteemed by (SEM/ EDX) of (JEOL JSM-6390LV). Infrared characterization, FTIR, was carried out to verify the existence of the Aurivillius phases in the prepared sample. For the electrical properties, both flat surfaces of the pellet were electroded with fine silver paint and kept at 200°C in an oven for 1 h prior to measurements. The dielectric permittivity and loss tangent of the sintered samples were measured as a function of frequency (1 kHz-1MHz) at different temperatures (RT to 700 °C) using the LCR meter in conjunction with a computer-controlled temperature chamber.

3 Results and Discussion

3.1 Structural Analysis

X-ray analysis (Figure 1) reveals that the powder in the two synthesis methods and crystallinity in the orthorhombic system with space group Fmmm indicates that the three layered perovskite structure of (ICSD: 98- 002- 4738) was preserved and no other impure phases appeared. Compared to pur BIT, the highest diffraction peak (117), which reveals that characteristic three-layer TiO_6 octahedra perovskite structure shifted gradually to a higher degree side (fom 30.168° to 30.27°). This displacement is due to the difference in the ionic radii of doping elements (Ni^{2+}: 0.69 Å and Ta^{5+}: 0.64 Å) at the Ti-site (Ti^{4+}: 0.605 Å) of the Aurivillius structure, thus, shrinkage to the crystal lattice [40].

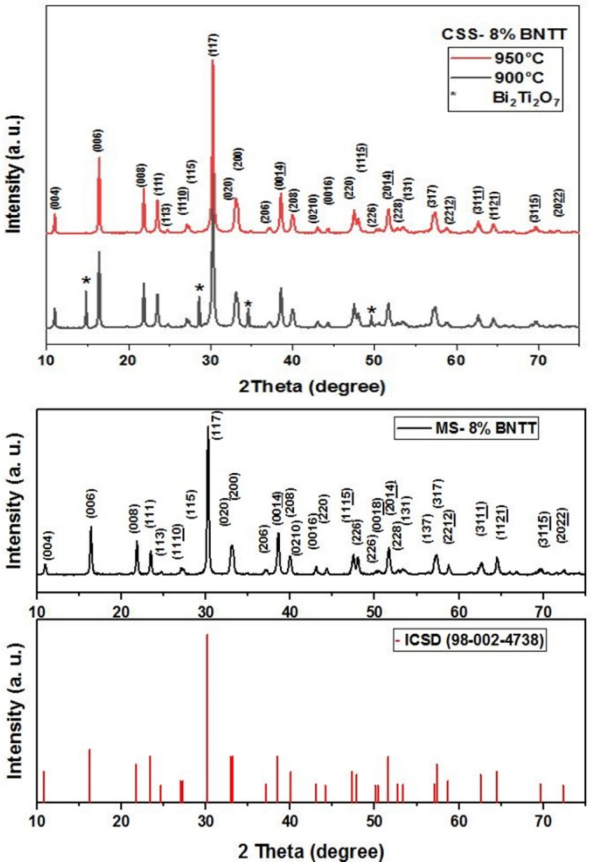

Fig. 1: X-ray indexed diffraction patterns of 8% BNTT synthesized by CSS and MS methods.

In addition (from Table 1), The CSS-8% BNTT sample had the largest crystallite size and cell volume, while MS-8% BNTT was the smallest. This relationship between the lattice parameter and crystallite size may be due to the thermodynamic state and surface stresses [41–44]
In addition, the Williamsson–Hall plot (Figure 2) reveals values close to the Scherrer relation. The average crystallite size was 52.3 nm, and 88.5 nm for CSS-8% BNTT and MS-8% BNTT, respectively.

3.2 Morphological Study

The observation of SEM micrographs of CSS- 8% BNTT and MS- 8% BNTT ceramics which are shown in Fig. 3 (a _b), and the use of "image J software" for the calculation of average particle size gives values around 25.46 µm and 1.18µm, respectively, for both samples. We can explain this big difference in values by the agglomeration of the crystallites to form the grain-likes [45].

Moreover, the dense morphology of the plate-like grains are, generally, due to the faster growth rate of grains along

the a-b plane than that along the c-axis in bismuth layer-structure materials [46, 47].

In addition, the energy dispersive X-ray spectrometer (EDX) analysis confirmed the purity of the samples prepared by both process (Fig. 3 (c _d)) because of the pics of all the stoichiometric elements Bi, Ti, Ni, Ta, and O.

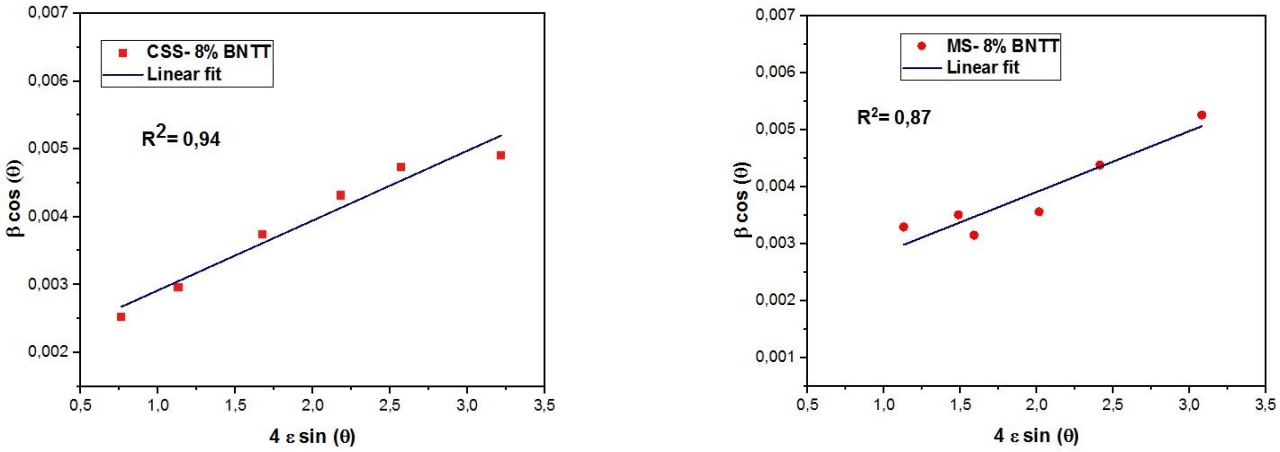

Fig. 2: Fitting plots of **β cosθ** versus **sinθ** in terms of Williamson-Hall equation.

Table 1: Structural end dielectric parameters of calcined samples.

	Lattice parameters in Å				Crystallite and grain size			Dielectric parameters 100kHz	
	a	b	c	V (Å^3)	Scherrer (nm)	W-H (nm)	SEM (µm)	T_c (°C)	ε max
BIT (98-002-4738)	5.4100	32.8400	5.4480	967.92					
CSS-8% BNTT	5.3993	32.8695	5.4459	966.49	40.79	52.3	25.46	696	9117,40
MS-8% BNTT	5.3989	32.8695	5.4405	965.46	37.58	88.5	1.18	666	7407,86

3.3 Fourier Transforms Infrared Spectroscopy (FTIR)

Infrared characterization, FTIR, was carried out to verify the existence of the Aurivillius structure in the prepared compound. There is a distinct band in the wave number range between 400 and 700 cm^{-1} FTIR spectra presented in Figure 4. For both methods and without any change, we note the presence of a strong peak at 570 cm^{-1} and peaks appearing in 838 cm^{-1} and 872 cm^{-1} are resulting from Ti–O/ or substituted Ti–O vibraching modes for the octahedral coordination TiO_6, which confirms the formation of the Aurivillius structure [48- 50].

3.4 Dielectric properties

Figure 5 illustrates the dielectric constant (ε') evolution of the two samples as a function of temperature. The highest Curie temperature (T_C) value was obtained at 696 °C for the CSS-8% BNTT ceramic, but MS-8% BNTT is obtained at 666 °C. According to H. Delavari and al. [51], the Curie temperature decreases with the minimized particles, this validates our work.

The frequency and temperature dependence of tangent loss (tanδ) of samples are shown in Fig. 6. With the increase in temperature, tanδ is found to be very low and almost remains constant, then beyond Tc indicates a significant increase. The nature of variation of tanδ at higher frequency and temperature can be explained by space-charge polarization [52]. The higher values of the loss tangent at high temperatures are attributed to the thermal conductivity losses, and similar behavior has been reported by other works [53].

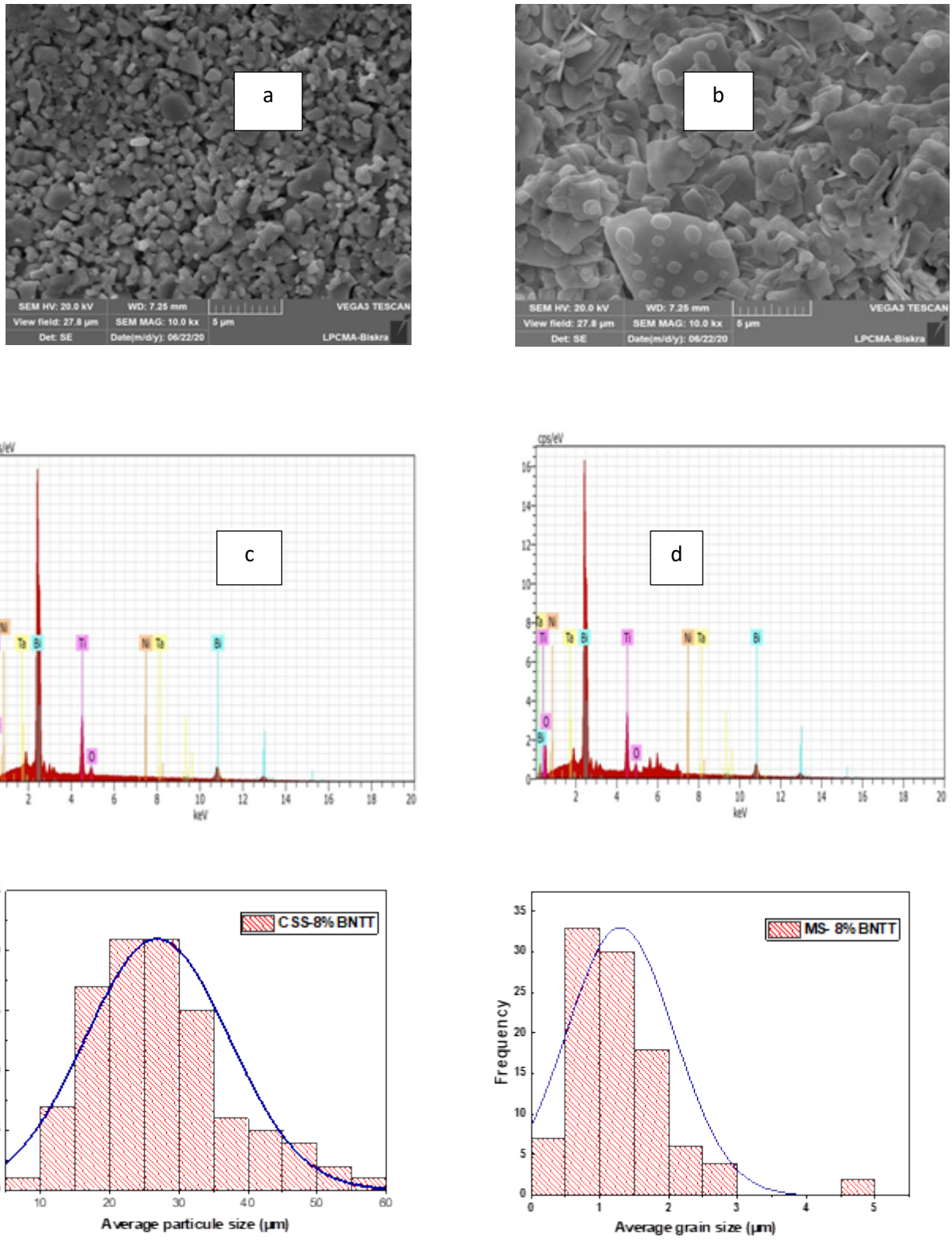

Fig. 3: a) and **b)** SEM micrographs, **c** and **d**) EDX analysis, and size distribution of the synthesized of samples CSS-8% BNTT and MS-8% BNTT, respectively

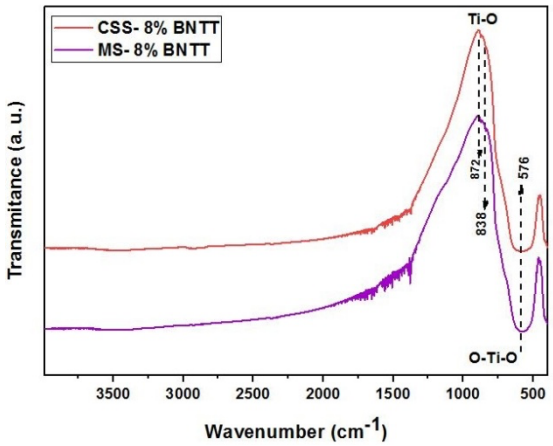

Fig. 4: FTIR spectra of synthesized compounds by CSS and MS methods.

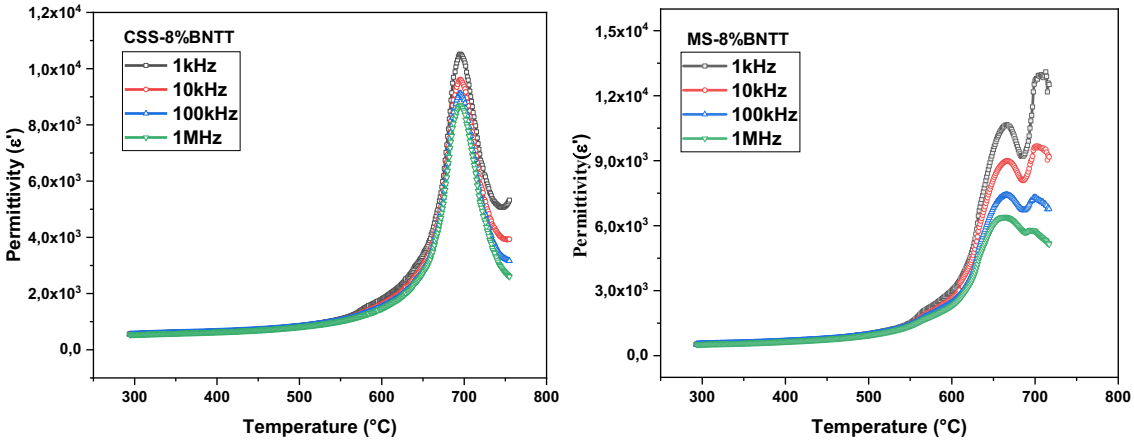

Figure 5: Temperature-frequency dependence of dielectric constant (ε') of CSS-8% BNTT and MS-8% BNTT

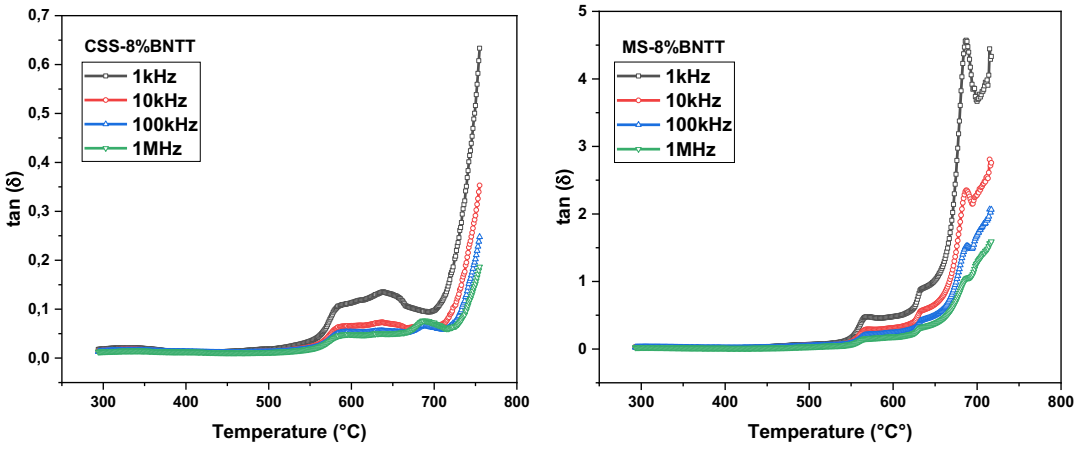

Fig. 6: Temperature-frequency dependence of dielectric loss (tan δ) of CSS-8% BNTT and MS-8% BNTT.

4 Conclusions

Polycrystalline powders with the composition of $Bi_4(Ni_{2/3}, Ta_{1/3})_{0.08}Ti_{2.92}O_{12}$ were prepared by conventional solide state reaction (CSS) and molten salt synthesis route (MS). It is clear from experimental results and discussion that the powders morphology and particles size can be modified by the variation in the synthesis route, and the following conclusions may possibly be drawn:

- X-ray diffraction (XRD) analysis reveals that the (Ni, Ta)-modified BIT ceramics have a pure orthorhombic three-layer Aurivillius type structure, but phase purity is obtained at two different temperatures, 950°C for CSS reaction, and at 850°C for MS method.

- The morphological study by SEM and EDX analysis confirms that the samples have a relatively dense pure, with micro-grains plate-like, structure typical for Aurivillius layered structures but strongly influenced by the crystallite size of both methods.

- By changing reaction method from CSS to MS, we found both the dielectric constant and tangent loss of 8% BNTT are decreased by increasing the curie temperature to high values.

Acknowledgement:

We thank Guesmi Brahim, from LPCMA-Biskra (Algeria), for his cooperation in the XRD and SEM/ EDX measurements. We also thank Khmakhem Hamdi (Laboratory of Multifunctional Materials and Applications, Tunisia) for his great help in dielectric measurements.

References

[1] B. Aurivillius, Mixed bismuth oxides with layer lattices II. Structure of Bi4Ti3O12 , Arkiv Kemi., **1**, 499-512 (1949).

[2] B. Aurivillius, Mixed bismuth oxides with layer lattices III. Structure of Ba Bi4Ti3O12, Arkiv Kemi., **2**, 519–527 (1950).

[3] E. C. Subbarao, A family of ferroelectric bismuth compounds, J. Phys. Chem. Solids., **23**, 665–676 (1965).

[4] E.C. Subbarao, Ferroelectricity in Bi4Ti3O12 and its solid solutions, Phys. Rev., **122**, 804 (1961).

[5] S.E. Cummins and L.E. Cross, Electrical and optical properties of ferroelectric Bi4Ti3O12 single crystals, J. Appl. Phys., **39**, 2268–2274 (1968).

[6] Y. Shimakawa, Y. Kubo, Y. Tauchi, H. Asano, T. Kamiyama, F. Izumi and Z. Hiroi, Crystal and electronic structures of Bi4-xLaxTi3O12 ferroelectric materials, Appl. Phys. Lett., **79**, 2791–2793 (2001).

[7] A. Fouskova and L.E. Cross, Dielectric properties of bismuth titanate, J. Phys. Chem. Solids., **23**, 2834 (1970).

[8] H. Yan, H. Zhang, R. Ubic, M. J. Reece, J. Liu, Z. Shen and Z. Zhang, A Lead-Free High-Curie-Point ferroelectric ceramic, CaBi2Nb2O9, J. Adv. Mater., **17**, 1261 (2005).

[9] A. Moure, A. Castro and L. Pardo, Aurivillius-type ceramics, a class of high temperature piezoelectric materials: drawbacks, advantages and trends, Prog. Solid State Chem., **37**, 15–39 (2009).

[10] V.A. Khomchenko, G.N. Kakazei, Y.G. Pogorelov, J.P. Araujo, M.V. Bushinsky, D.A. Kiselev, A.L. Kholkin and J.A. Paixão, Effect of Gd substitution on ferroelectric and magnetic properties of Bi4Ti3O12, Mater. Lett., **64**, 1066–1068 (2010).

[11] J. Paul, S. Bhardwaj, K.K. Sharma, R.K. Kotnala and R. Kumar, Room temperature multiferroic behaviour and magnetoelectric coupling in Sm/Fe modified $Bi_4Ti_3O_{12}$ ceramics synthesized by solid state reaction method, *J. Alloy. Compd.*, **634**, 58–64 (2015).

[12] J. Paul, S. Bhardwaj, K.K. Sharma, R.K. Kotnala and R. Kumar, Room-temperature multiferroic properties and magnetoelectric coupling in $Bi_{4-x}Sm_xTi_{3-x}Co_xO_{12-d}$ ceramics, *J. Mater. Sci.,* **49**, 6056–6066 (2014).

[13] J. Paul, S. Bhardwaj, K.K. Sharma, R.K. Kotnala and R. Kumar, Room temperature multiferroic properties and magnetoelectric coupling in Sm and Ni substituted $Bi_{4-x}Sm_xTi_{3-x}Ni_xO_{12\pm d}$ (x = 0, 0.02, 0.05, 0.07) ceramics, *J. Appl. Phys.*, **115**, 204–909 (2014).

[14] A. Megriche, L. Lebrun and M. Troccaz, Materials of $Bi_4Ti_3O_{12}$ type for high temperature acoustic piezo-sensors, Sensors Actuators, *A. Phys.*, **78**, 88–91 (1999).

[15] B.H. Park, B.S. Kang, S.D. Bu, T.W. Noh, J. Lee and W. Jo, Lanthanum-substituted bismuth titanate for use in non-volatile memories, Nature., **401**, 682–684 (1999).

[16] H. Qi, Y. Qi and M. Xiao, Leakage mechanisms in rare-earth (La, Nd) doped Bi4Ti3O12 ferroelectric ceramics, J. Mater. Sci., **25**, 1325–1330 (2014).

[17] ReYuji Noguchi, Masaru Miyayama and Tetsuichi Kudo, Direct evidence of A-site deficient strontium bismuth tantalate and its enhanced ferroelectric properties, Phys. Rev., **B 63 (21)**, 214102–214108 (2001).

[18] H. Du, L. Tang, and S. Kaskel, Preparation, Microstructure and ferroelectric properties of Bi3.25La0.75Ti3−xMxO12 (M = Mo, W, Nb, V) Ceramics, J. Phys. Chem., **C113**, 1329 (2009).

[19] Ruixia Ti, Chaoyang Wang, Huarui Wu, Yan Xu and Chenyang Zhang, Study on the structural and magnetic properties of Fe/Co co-doped Bi4Ti3O12 ceramics, Ceramics International., **45**, 7480–7487 (2019).

[20] B. Yuan, J. Yang, J. Chen, X.Z. Zuo, L.H. Yin, X.W. Tang, X.B. Zhu, J.M. Dai, W.H. Song, Y.P. Sun, Magnetic and dielectric properties of Aurivillius phase Bi6Fe2Ti3-2xNbxCoxO18 (0 = x = 0.4), Appl. Phys. Lett., **104**, 062413 (2014).

[21] J.G. Hou, R.V. Kumar, Y.F. Qu and D. Krsmanovic, B-site doping effect on electrical properties of Bi4Ti3-2xNbxTaxO12 ceramics, Scripta Mater., **61**, 664–667 (2009).

[22] J. Hou, Y. Qu, R. Vaish, K.B.R. Varma, D. Krsmanovic and R.V. Kumar, Crystallographic evolution, dielectric, and piezoelectric properties of Bi4Ti3O12 :W/Cr ceramics, J. Am. Ceram. Soc., **93**, 1414–1421 (2010).

[23] Y. Chen, D. Liang, Q. Wang, J. Zhu, Microstructures, dielectric, and piezoelectric properties of W/Cr co-doped Bi4Ti3O12 ceramics, J. Appl. Phys., **116**, 074108 (2014).

[24] Y. Chen, Z. Peng, Q. Wang and J. Zhu, Crystalline structure, ferroelectric properties, and electrical conduction characteristics of W/Cr co-doped Bi4Ti3O12 ceramics, J. Alloys Compd., **612**, 120–125 (2014).

[25] P. Siriprapa, A. Watcharapasorn and S. Jiansirisomboon, Structure-property relations of co-doped bismuth layer-structured Bi3.25La0.75(Ti1-xMox)3O12 ceramics, Nanoscale Research Letters., **7**, 42 (2012).

[26] R. J. Koch, I.N. Lokuhewa, J. Shi, M.S. Haluska and S.T. Misture, Chemical synthesis of nanoscale Aurivillius ceramics, Bi2A2TiM2O12 (A=Ca, Sr, Ba and M=Nb, Ta), J. Sol. Gel. Sci. Technol., **64**, 612–618 (2012).

[27] Y. Chen, S. Xie, Q. Wang and J. Zhu, Influence of Cr2O3 additive and sintering temperature on the structural characteristics and piezoelectric properties of Bi4Ti2.95W0.05O12.05 Aurivillius ceramics, Progress in Natural Science: Materials International., **26**, 572–578 (2016).

[28] C. Lavado and M.G. Stachiotti, Fe3+/ Nb5+ co-doping effects on the properties of Aurivillius Bi4Ti3O12 ceramics, Journal of Alloys and Compounds., **731**, 914–919 (2018).

[29] T. Wei, F. Yang, B. Jia, C. Zhao, L. Liu, H. Zhang, X. Yan and J. Yang, Reversible photoluminescence modulation in praseodymium-doped bismuth titanate ceramics for information storage based on photochromic reaction, Ceramics International., **46**, 18507–18517 (2020).

[30] D.Y. Guo, C.Y. Liu, C.B. Wang, Q. Shen, and L.M. Zhang, A Review of one-dimensional TiO2 nanostructured materials for environmental and Energy Applications, J. Mater. Sci: Mater. El., **22**, 130 (2011).

[31] R. Wisedsri, T. Chaisuwan and S. Wongkasemjit, Simple route to bismuth titanate from bismuth glycolate precursor via sol–gel process, Mater. Res. Innov., **17**, 43–48 (2013).

[32] MS. Haluska, S. Speakman and ST. Misture, In situ XRD to optimize powder synthesis of Aurivillius phases., Adv. X-Ray Anal., **45**, 110–116 (2002).

[33] Y. Kan, X. Jin, P. Wang, Y. Li, Y.B. Cheng and D. Yan, Anisotropic grain growth of Bi4Ti3O12 in molten salt fluxes, Mater. Res. Bull., **38**, 567– 576 (2003).

[34] Q.Y. Tang, Y.M. Kan, P.L. Wang, Y.G. Li, G.J. Zhang, Nd/V co-doped Bi4Ti3O12 powder prepared by molten salt synthesis, J. Am. Ceram. Soc., **90**, 3353–3356 (2007).

[35] H. He, J. Yin, Y. Li, Y. Zhang, H. Qiu, H. Xu, T. Xu and C. Wang, Size controllable synthesis of single-crystal ferroelectric Bi4Ti3O12 nanosheet dominated with {0 0 1} facets toward enhanced visible-light-driven photocatalytic activities, Appl. Catal. **B156**, 35–43 (2014).

[36] H. Hao, H. Liu, Y. Liu, M. Cao and S. Ouyang, Lead-Free SrBi4Ti4O15 and Bi4Ti3O12 material fabrication using the microwave-assisted molten salt synthesis method, J. Am. Ceram. Soc., **90**, 1659–1662 (2007).

[37] Chao Jiang, Kechao Zhou, Xuefan Zhou, Zhiyou Li and Dou Zhang, Synthesis and characterization of Na0.5Bi0.5TiO3 platelets with preferred orientation using Aurivillius precursors, Ceramics International, 41, 6858–6862 (2015).

[38] T. Kimura and T. Yamaguchi, Fused salt synthesis of Bi4Ti3O12, Ceramics International., **9**, 13-17 (1983).

[39] E. M. Benali, A. Benali, M. Beiar, E. Dhahri, M. P. F. Graca, M. A. Valense and B. F. O. Cossa, Effect of synthesis route on structural, morphological, Raman, dielectric and electric properties of La0.8Ba0.1Bi0.1FeO3, Journal of Materials Science: Materials in Electronics., **31**, 3197–3214 (2020).

[40] R.D. Shannon, Revised effective ionic radii and systematic studies of interatomic distances in halides and chalcogenides, Acta Crystallogr.- Sect. A Cryst. Phys. Diffr. Theor. Gen. Crystallogr., **32(5)**, 751–767 (1976).

[41] W. H. Qi and M. P. Wang, Size and shape dependent lattice parameters of metallic nanoparticles, J. Nanopart. Res., **7(1)**, 51 (2005).

[42] M. Kezrane, A. Guittoum, M. Hemmous, S. Lamrani, A. Bourzami and W. Weber, Elaboration, microstructure and magnetic properties of nanocrystalline Fe90Ni10 powders, J. Supercond. Novel Magn., **28(8)**, 2473 (2015).

[43] G. K. Rane, U. Welzel, S. R. Mekaa, and E. J. Mittemeijer, Non-monotonic lattice parameter variation with crystallite size in nanocrystalline solids, Acta Mater., **61(12)**, 4524 (2013).

[44] M. L. Sui and K. Lu, Variation in lattice parameters with grain size of a nanophase Ni3P compound, Mater. Sci. Eng. A, **179-180(1)**, 541–544 (1994).

[45] Y. Köseo lu, E. entürk, V. Eyüpo lu, T. Kuru, M. Hashim and S. S. Meena, J. Supercond. Nov. Magn., **29**, 2813–2819 (2016).

[46] L. Yu, J. D. Hao, Z. J. Xu, W. Li, R. Q. Chu and G. R. Li, Strong red emission and enhanced ferroelectric properties in (Pr, Ce)-modified Na0.5Bi4.5Ti4O15 multifunctional ceramics, J. Mater. Sci. Mater. Electron., **27**, 12216–12221 (2016).

[47] F. Liu, X. P. Jiang, C. Chen, X. Nie, X. K. Huang, Y. J. Chen, H. Hu and C. Y. Su, Structural, electrical and photoluminescence properties of Er3+-doped SrBi4Ti4O15 - Bi4Ti3O12 inter-growth ceramics, Mater. Sci., **13**, 99–106 (2019).

[48] D. Chen and X. Jiao, Hydrothermal synthesis and characterization of Bi4Ti3O12 powders from different precursors, Mater. Res. Bull., **36**, 355–363 (2001).

[49] Y. Kan, P. Wang, Y. Li, Y.B. Cheng and D. Yan, Low-temperature sintering of Bi4Ti3O12 derived from co-precipitation method, Mater. Lett., **56**, 910–914 (2002).

[50] R. Anlin Golda, A. Marikani and D. Pathinettam Padiyan, Mechanical synthesis and characterization of Bi4Ti3O12 nanopowders, Ceramics International., **37**, 3731–3735 (2011).

[51] H. Delavari, H. M. Hosseini, and A. Simchi, A simple model for the size and shape dependent Curie temperature of free standing Ni and Fe nanoparticles based on the average coordination number and atomic cohesive energy, Chem. Phys., **383(1- 3)**, 1-5 (2011).

[52] L. Mrharrab and A. Elbasset, The study of anomalies in the

PZT material, International Journal of Development Research., **5 (10)**, 5699–5703 (2015).

[53] D. K. Pradhan, R. N. P. Chowdhury, T. K. Nath, Magnetoelectric properties of PbZr0.53Ti0.47O3–Ni0.65Zn0.35Fe2O4 multiferroic nanocomposites, Appl Nanosci., **2**, 261–273 (2012).